Eur Radiol (2014) 24:1878–1888
DOI 10.1007/s00330-014-3199-5

CARDIAC

Reproducibility of aortic annulus measurements by computed tomography

Annika Schuhbaeck · Stephan Achenbach · Tobias Pflederer · Mohamed Marwan · Jasmin Schmid · Holger Nef · Johannes Rixe · Franziska Hecker · Christian Schneider · Michael Lell · Michael Uder · Martin Arnold

Received: 24 October 2013 / Revised: 8 April 2014 / Accepted: 23 April 2014 / Published online: 22 May 2014

Abstract
Objectives To evaluate a systematic approach for measurement of aortic annulus dimensions by cardiac computed tomography.
Methods CT data sets of 64 patients were evaluated. An oblique cross-section aligned with the aortic root was created by systematically identifying the caudal insertion points of the three aortic cusps and sequentially aligning them in a double oblique plane. Aortic annulus dimensions, distances of coronary ostia and a suitable fluoroscopic projection angle were independently determined by two observers.
Results Interobserver intraclass correlation coefficients (ICC) for aortic annulus diameters were excellent (ICC 0.89–0.93). Agreement for prosthesis size selection was excellent (κ=0.86 for mean, κ=0.84 for area-derived and κ=0.91 for circumference-derived diameter). Mean distances of the left/right coronary ostium were 13.4±2.4/14.4±2.8 mm for observer 1 and 13.2±2.7/13.5±3.2 mm for observer 2 (p=0.30 and p=0.0001, respectively; ICC 0.76/0.77 for left/right coronary artery). A difference of less than 10° for fluoroscopic projection angle was achieved in 84.3 % of patients.
Conclusions A systematic approach to generate a double oblique imaging plane exactly aligned with the aortic annulus demonstrates high interobserver and intraobserver agreements for derived measurements which are not influenced by aortic root calcification.
Key Points
- *Systematic approach to generate a double oblique imaging plane for TAVI evaluation.*
- *This method is straightforward and software independent.*
- *An approach with high reproducibility, not influenced by aortic root calcification.*

Keywords Aortic valve stenosis · Heart valve prosthesis implantation · Multidetector computed tomography · Cardiac imaging techniques · Imaging · Three-dimensional

A. Schuhbaeck (✉) · S. Achenbach · T. Pflederer · M. Marwan · J. Schmid · M. Arnold
Department of Cardiology, University of Erlangen, Ulmenweg 18, 91054 Erlangen, Germany
e-mail: annika.schuhbaeck@uk-erlangen.de

A. Schuhbaeck · S. Achenbach · H. Nef · J. Rixe · F. Hecker
Department of Cardiology, University of Gießen, Gießen, Germany

C. Schneider
Department of Radiology, University of Gießen, Gießen, Germany

M. Lell · M. Uder
Department of Radiology, University of Erlangen, Erlangen, Germany

Introduction

For transcatheter aortic valve implantation (TAVI), accurate measurement of aortic annulus dimensions and the distances of coronary ostia from the aortic valve plane are essential to minimize procedure-associated complications such as annular rupture, embolization of the prosthesis, obstruction of coronary ostia or paravalvular aortic regurgitation [1–5]. Multidetector computed tomography (CT) permits the measurement of aortic annulus parameters in the work-up of TAVI candidates, improves the accuracy of aortic annulus sizing over echocardiography and potentially reduces the incidence of paravalvular regurgitation and other complications [6–12]. Several methods have been suggested to measure aortic annulus dimensions by CT. They include creating a coronal and sagittal oblique plane, an oblique plane in a three-chamber view or a double oblique transverse imaging plane of the basal ring [6, 13].

If the aortic valve plane is accurately defined in computed tomography, it is possible to predict fluoroscopic projection angles which provide an orthogonal view on the valve plane [14–17]. This may minimize the number of required aortograms and reduce the amount of contrast needed for the procedure [17]. Inter- and intraobserver variability of methods to predict fluoroscopic projection angles have not yet been systematically evaluated.

Our objective was to evaluate a systematic method to create a double oblique imaging plane exactly aligned with the aortic annulus and to determine its reproducibility regarding measurement of aortic annulus parameters, the distances of the coronary ostia from the aortic valve plane and a suitable fluoroscopic projection angle.

Our hypothesis was that this systematic approach should yield high interobserver agreement of measurements required for the workup of TAVI candidates.

Materials and methods

Sixty-four consecutive patients with severe aortic valve stenosis who were referred for dual source CT for routine evaluation before TAVI were included. Medication for heart rate reduction or nitrates were not used prior to CT data acquisition because evaluation of the coronary arteries was not the primary goal.

Imaging was performed in deep inspiration in a craniocaudal direction beginning at the aortic arch and ending at a level below the hips. Tube voltage and tube current were selected depending on patient size (100 kV tube voltage for patients with a body weight no greater than 100 kg and 120 kV in larger patients).

In 12 patients, imaging was performed on a first-generation dual source CT (Somatom Definition, Siemens Healthcare, Forchheim, Germany, 300 ms rotation, 2×64×0.6 mm collimation) with retrospectively electrocardiogram (ECG)-gated spiral acquisition and ECG-gated dose modulation (35–70 % of the R–R interval). The amount of contrast agent was selected on the basis of patient size (100–120 ml of Iopromide, Ultravist 370, Bayer Pharma AG, Berlin, Germany) and was injected at a flow rate of 3.0 to 4.5 ml/s followed by 50 ml of saline at the same flow rate. Bolus tracking with a region of interest placed in the ascending aorta and a preset threshold of 170 Hounsfield units (HU) was used.

In 52 patients, imaging was performed on a second-generation dual source CT (Definition Flash, Siemens Healthcare, Forchheim, Germany, 280 ms rotation, 2×128×0.6 mm collimation) using either a retrospectively ECG-gated spiral acquisition mode with ECG-gated tube current modulation (n=24) or prospectively ECG-triggered high-pitch spiral acquisition starting the examination so that data acquisition in a "cardiac-specific window" would be initiated at 60 % of the R–R interval (n=28). A timing bolus protocol was used as previously described [18], with a region of interest placed in the descending abdominal aorta to avoid outrunning the bolus by high pitch acquisition.

CT image reconstruction

Transaxial CT data sets ranging from the aortic arch to the diaphragm were reconstructed with 0.6 mm slice thickness, increment of 0.3 mm and a medium smooth reconstruction kernel ("B26f"). In retrospectively ECG-gated spiral acquisition, an automatic reconstruction algorithm selected the optimal phase for image reconstruction (in most cases between 70 % and 75 % of the R–R interval).

Systematic approach to obtain a multiplanar reconstruction exactly aligned with the aortic annulus

Multiplanar reconstructions to obtain an image plane exactly aligned with the aortic annulus were performed as previously reported [19]. Images were transferred to an offline workstation (Siemens Multimodality Work Place, Siemens Healthcare, Forchheim, Germany) equipped with a software package (Circulation, Siemens Healthcare, Forchheim, Germany) which allowed free manipulation of multiplanar reconstructions. Data analysis was performed by two observers. One observer had more than 10 years' experience and the other observer had 3 years' experience in cardiac CT. Both observers were blinded to each other's measurement results.

Aortic annulus dimensions

The minimum and maximum diameter, area and circumference of the aortic annulus were manually traced (Fig. 1). The mean diameter of the aortic annulus was obtained by calculating the mean of the minimum and maximum diameters of the aortic annulus [11, 20].

The area-derived diameter D_a of the aortic annulus was calculated using the following formula:

$$D_a = 2\sqrt{\frac{Area}{\pi}}$$

[6]

The circumference-derived diameter D_c of the aortic annulus was calculated using the following formula:

$$D_c = \frac{Circumference}{\pi}$$

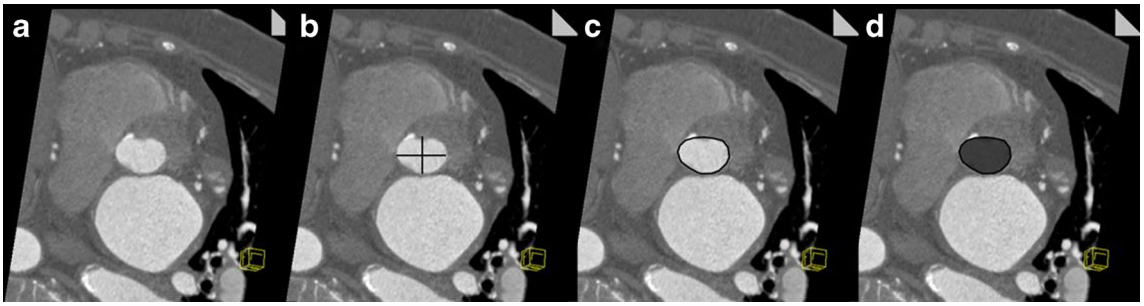

Fig. 1 Measurement of the aortic annulus parameters in an 88-year-old female patient with severe aortic valve stenosis. **a** Multiplanar reconstruction exactly aligned with the aortic annulus. **b** Measurement of minimal and maximal diameter of the aortic annulus. **c** Measurement of the circumference of the aortic annulus. **d** Measurement of the area of the aortic annulus

Aortic root calcification

To analyse the extent of aortic root calcification, a maximum intensity projection (MIP) with a slice thickness of 5 mm was created at the position of the aortic valve plane. The extent of calcification was visually graded using a scale from 0 to 4 (Fig. 2).

Distance of coronary ostia from the aortic annulus plane

Once the double oblique image aligned with the aortic annulus was created, coronary ostia were identified by moving the imaging plane in a cranial direction until the ostium of the left main or right coronary artery appeared. Reference lines were then positioned on the coronary ostium and rotated so that the distance of the coronary artery from the aortic valve plane could be measured in the formerly sagittal or coronal plane (Fig. 3).

Measuring the potential fluoroscopic projection angle

After creating the double oblique image aligned with the aortic annulus, we moved the plane in a cranial direction until the commissures of all three valve cusps could be identified. The centre point of the reference lines was positioned in the coaptation point of all three commissures and rotated so that the formerly coronal plane was in a left anterior oblique (LAO) 10° orientation (Fig. 4). The corresponding cranial or caudal direction was noted. LAO 10° orientation was selected to ensure comparability between the measurements of both observers.

Analysis time

The time to align the imaging plane with the aortic annulus as well as the time for the entire analysis (including aortic annular parameters, distances of the coronary ostia from the aortic valve plane and the potential fluoroscopic projection angle) was measured in all patients.

Interobserver and intraobserver agreement regarding prosthesis size selection

The interobserver and intraobserver agreement of prosthesis size selection according to measured aortic annulus parameters was determined. We used a sizing model according to Gurvitch et al. [6]: A 23-mm valve is suggested for mean aortic annulus diameters of 19.5–22.5 mm, a 26-mm valve for greater than 22.5 to 26.5 mm, a 29-mm valve for greater than 26.5 to 29.5 mm and aortic annulus parameters exceeding 29.5 mm were regarded as too large for TAVI.

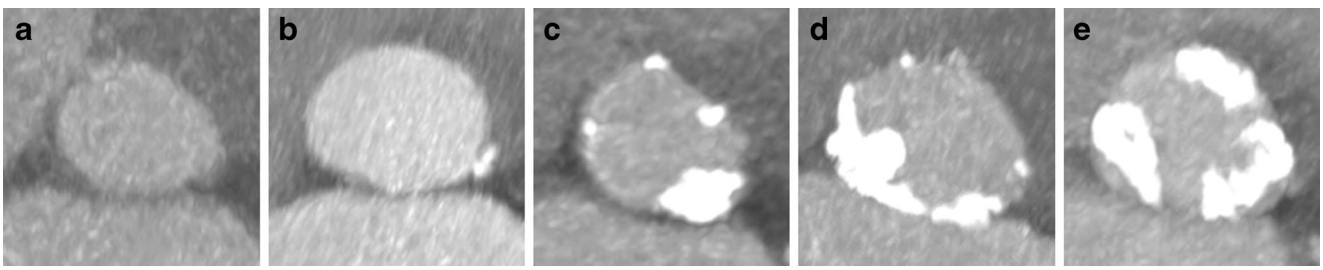

Fig. 2 Analysis of aortic root calcification in maximum intensity projections with a slice thickness of 5 mm. **a** 0=no calcification. **b** 1=calcification≤25 % of the circumference. **c** 2=calcification of 25–49 % of the circumference. **d** 3=calcification of 50–75 % of the circumference. **e** 4=calcification exceeding 75 % of the circumference

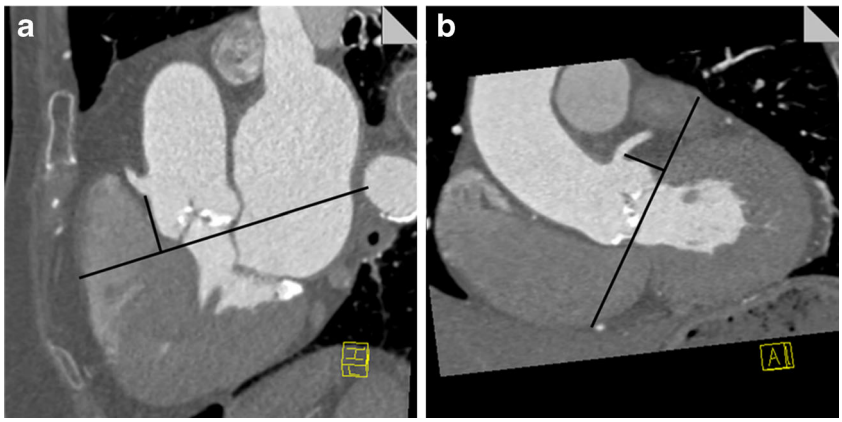

Fig. 3 Measurement of the distances from the coronary ostia to the aortic annulus plane in an 88-year-old female patient with severe aortic valve stenosis. **a** Measurement of the distance of the right coronary artery from the aortic valve plane (18 mm). **b** Measurement of the distance of the left main coronary artery from the aortic valve plane (12 mm)

Statistical analysis

Statistical analyses were performed using Microsoft Excel (2010), Graph Pad Prism Version 5.01 (Graph Pad Software, San Diego California, USA) and PASW Statistics version 18 (SPSS, Inc., an IBM Company, Chicago, Illinois, USA). Continuous variables are expressed as mean ± SD; categorical variables as frequencies or percentages. For continuous variables, a two-sided Wilcoxon signed rank test was used for paired observations and a Mann–Whitney *U* test for unpaired observations. *P* values less than 0.05 were considered to be statistically significant. Bland–Altman analysis was performed to compare intra- and interobserver results. Comparison of categorical variables was performed using a chi-square analysis. Intraclass correlation coefficients (ICC) were determined to compare aortic annulus dimensions, distances of the coronary ostia from the annulus and the potential fluoroscopic projection angle. ICC was defined as the ratio of between-subject variance to the total variance. The 95 % confidence intervals (CI) were also calculated. Weighted Cohen's kappa coefficients (κ values) were calculated for the assessment of interobserver and intraobserver agreements on valve size selection. ICC values and κ values were interpreted as follows: absence of agreement, 0 or less; poor agreement, less than 0.20; fair agreement, 0.21–0.40; moderate agreement, 0.41–0.60; good agreement, 0.61–0.80; and excellent agreement, greater than 0.80 [21].

Results

Baseline characteristics

The patients' mean age was 83±4 years (range 72–94 years). Of all 64 patients, 29 were male (45 %) and 35 (55 %) were female. The mean logistic Euroscore was 32.6±14.0 % (range 6.6–73.8 %). Consecutive patients were evaluated and no data sets were excluded for reduced image quality.

Aortic annulus dimensions: intraobserver agreement

Mean differences between the two measurements were 0.4± 0.9 mm for the mean diameter, 0.4±0.8 mm for the circumference-derived diameter and 0.6±0.8 mm for the

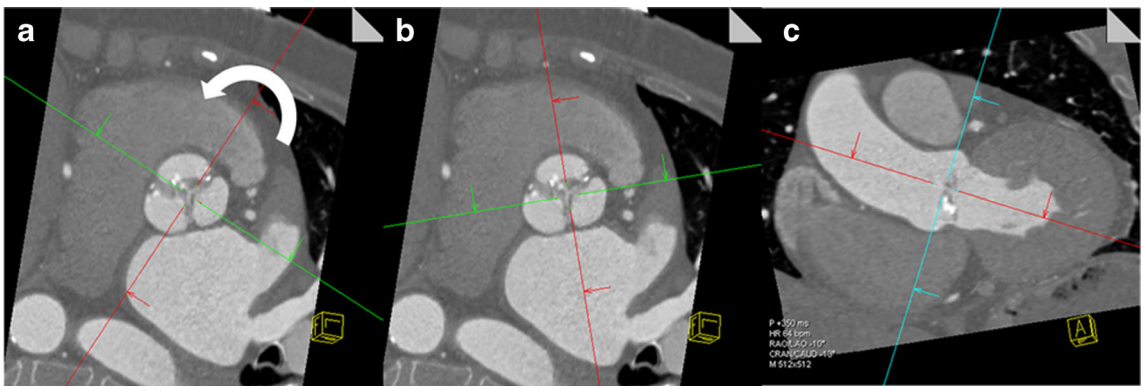

Fig. 4 Measurement of the potential fluoroscopic projection angle in an 88-year-old female patient with severe aortic valve stenosis. After creation of a double oblique image showing all three valve cusps, the centre point of the reference lines was positioned in the centre of all three commissures (**a**) and rotated so that the formerly coronal plane was in an LAO 10° orientation (**b**). The corresponding cranial or caudal direction was noted in the coronal plane (**c**). In this case, the potential fluoroscopic projection angle at LAO 10° would be caudal 13°

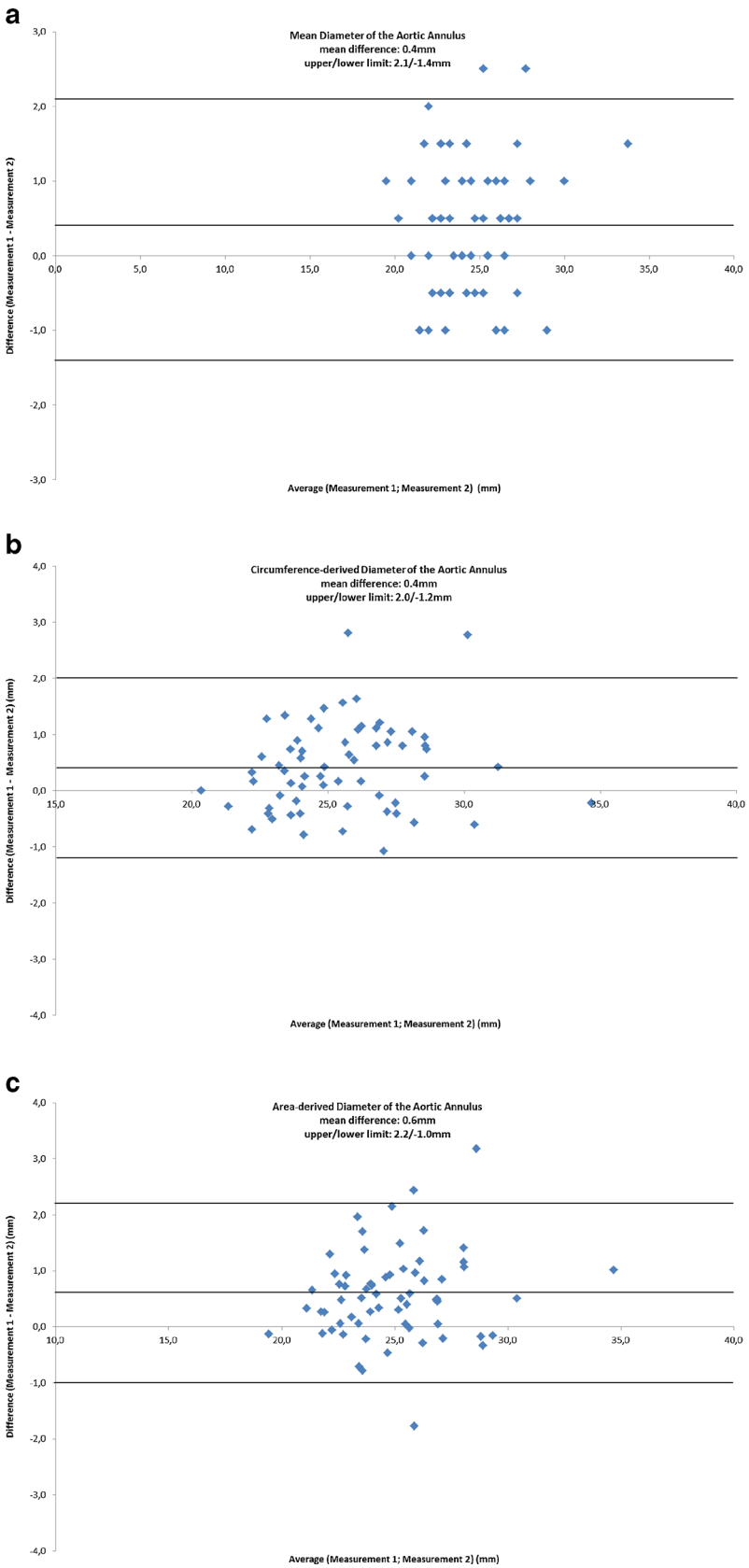

Fig. 5 Bland–Altman analysis of intraobserver measurements of the mean diameter (**a**), circumference-derived diameter (**b**) and the area-derived diameter (**c**)

Table 1 Intraobserver results of the aortic annulus parameters, distances of the coronary ostia from the aortic valve plane and the suggested fluoroscopic projection angle

	Measurement 1	Measurement 2	Significance (*p* value)
Intraobserver			
Short diameter (mm)	21.7±2.6	21.3±2.4	0.005
Long diameter (mm)	27.5±3.1	27.2±3.0	n.s. (0.09)
Mean diameter (mm)	24.6±2.6	24.2±2.5	0.03
Area-derived diameter (mm)	25.2±2.7	24.7±2.5	<0.0001
Circumference-derived diameter (mm)	25.7±2.6	25.3±2.5	0.0001
Distance to LM (mm)	13.4±2.4	13.3±2.3	n.s. (0.79)
Distance to RCA (mm)	14.4±2.8	15.1±3.0	0.001
Cranio-caudal orientation of a suitable fluoroscopic plane at LAO 10°	−5.3±12.9	−4.3±13.7	n.s. (0.06)

Cranial +, caudal −

area-derived diameter. Maximum differences were 2.5 mm for the mean diameter, 2.8 mm for the circumference-derived diameter and 3.2 mm for the area-derived diameter (Fig. 5). Intraobserver results of the aortic annulus dimensions, distances of the coronary ostia from the aortic annulus and the fluoroscopic projection angle are shown in Table 1. Intraobserver reliability for all aortic annulus dimensions was excellent with an ICC between 0.89 and 0.94 (Table 2).>

Aortic annulus dimensions: interobserver agreement

Bland–Altman analysis revealed a mean difference between the two observers of −0.2±1.1 mm for the mean diameter, 0.2 ±1.1 mm for the circumference-derived diameter and 0.4± 0.9 mm for the area-derived diameter. The maximum difference was 4.5 mm for the mean diameter, 6.7 mm for the circumference-derived diameter and 5.6 mm for the area-derived diameter (Fig. 6).

The minimum, maximum and mean diameters as well as the circumference-derived diameter D_c did not differ significantly between the two observers (Table 3). Interobserver agreement was excellent for the minimum (ICC 0.89, 95 % CI 0.83–0.93), the maximum (ICC 0.90, 95 % CI 0.84–0.94) and the mean diameter of the aortic annulus (ICC 0.92, 95 % CI 0.87–0.95) as well as the circumference-derived diameter (ICC 0.91, 95 % CI 0.86–0.95, Table 2). There was a slight but significant difference for the area-derived diameter of the aortic annulus between both observers (25.2±2.7 vs. 24.8± 2.5 mm, $p<0.0001$). Interobserver agreement was excellent (ICC 0.93, 95 % CI 0.85–0.96 for area-derived diameter).

Distances of the coronary ostia from the aortic annulus plane: intraobserver agreement

The distance of the left main coronary artery from the aortic annulus plane was not significantly different for the two measurements (13.4±2.4 vs. 13.3±2.3 mm, $p=0.79$). However, the results were significantly different for the right coronary artery (14.4±2.8 vs. 15.1±3.0 mm, $p=0.001$). Intraobserver reliability was excellent for the left main (ICC 0.82, 95 % CI 0.72–0.89) and right coronary artery (ICC 0.81, 95 % CI 0.68–0.89).

Distances of the coronary ostia from the aortic annulus plane: interobserver agreement

The distance of the left main coronary artery from the aortic annulus plane was not different between the observers (13.4± 2.4 vs. 13.2±2.7 mm, $p=0.30$). However, the distance of the right coronary artery from the aortic annulus plane

Table 2 Interobserver and intraobserver correlation of the aortic annulus parameters, distances of the coronary ostia from the aortic valve plane and the suggested fluoroscopic projection angle

	Interobserver (ICC, 95 % CI)	Intraobserver (ICC, 95 % CI)
Short diameter (mm)	0.89 (0.83–0.93)	0.89 (0.80–0.93)
Long diameter (mm)	0.90 (0.84–0.94)	0.89 (0.83–0.93)
Mean diameter (mm)	0.92 (0.87–0.95)	0.93 (0.87–0.96)
Area-derived diameter (mm)	0.93 (0.85–0.96)	0.93 (0.78–0.93)
Circumference-derived diameter (mm)	0.91 (0.86–0.95)	0.94 (0.87–0.97)
Distance to LM (mm)	0.76 (0.64–0.85)	0.82 (0.72–0.89)
Distance to RCA (mm)	0.77 (0.58–0.87)	0.81 (0.68–0.89)
Projection angle LAO 10°	0.81 (0.70–0.88)	0.83 (0.74–0.90)

ICC intraclass correlation coefficient, *CI* confidence interval

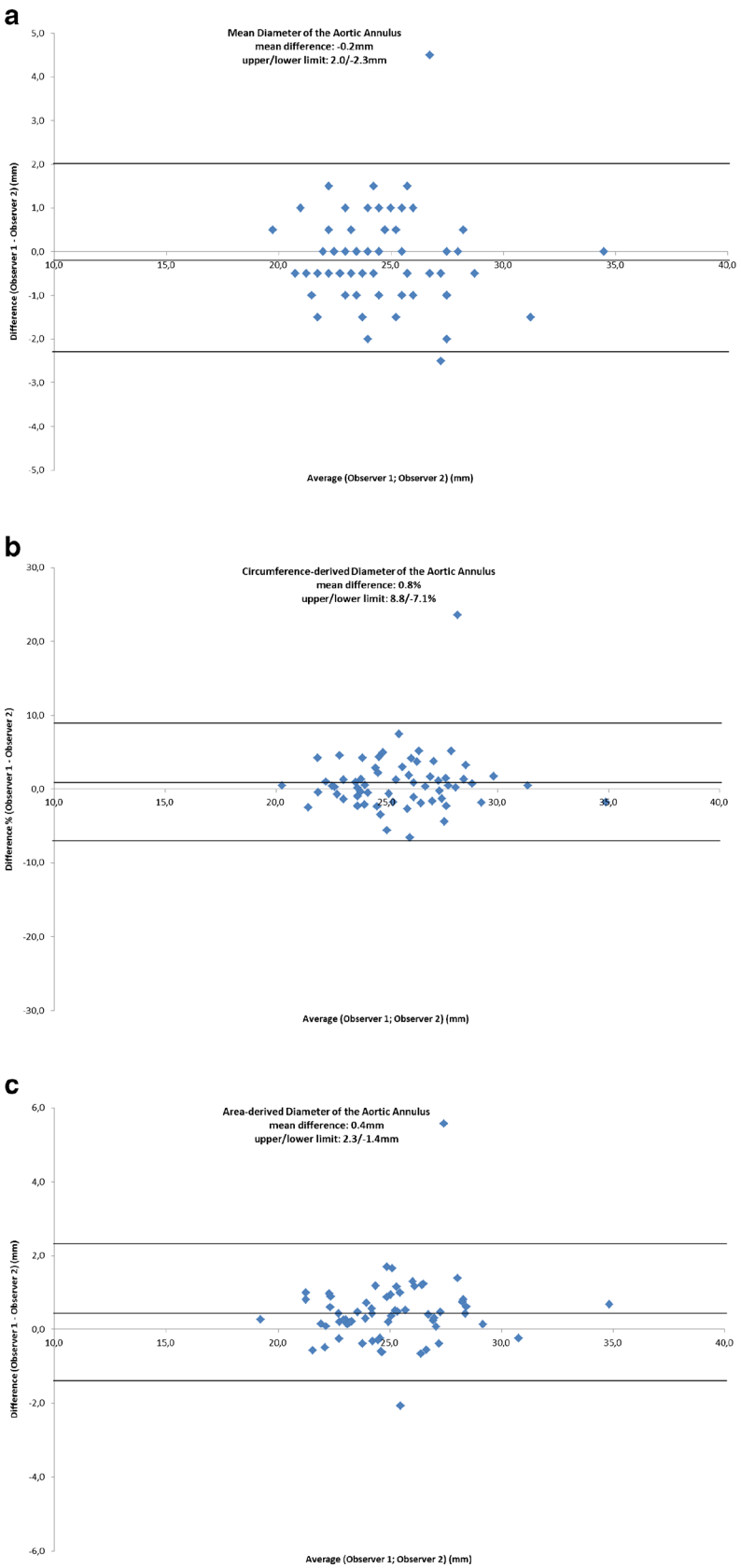

Fig. 6 Bland–Altman analysis of interobserver measurements of the mean diameter (**a**), circumference-derived diameter (**b**) and the area-derived diameter (**c**)

Table 3 Interobserver results of the aortic annulus dimensions, distances of the coronary ostia from the aortic annulus plane and the suggested fluoroscopic projection angle

	Observer 1	Observer 2	Significance (p value)
Interobserver			
Short diameter (mm)	21.7±2.6	22.0±2.7	n.s. (0.06)
Long diameter (mm)	27.5±3.1	27.5±3.1	n.s. (0.57)
Mean diameter (mm)	24.6±2.6	24.8±2.7	n.s. (0.13)
Area-derived diameter (mm)	25.2±2.7	24.8±2.5	<0.0001
Circumference-derived diameter (mm)	25.7±2.6	25.5±2.5	n.s. (0.19)
Distance to LM (mm)	13.4±2.4	13.2±2.7	n.s. (0.30)
Distance to RCA (mm)	14.4±2.8	13.5±3.2	0.0001
Cranio-caudal orientation of a suitable fluoroscopic plane at LAO 10°	−5±13	−7±14	n.s. (0.22)

Cranial +, caudal −

was significantly different (14.4±2.8 vs. 13.5±3.2 mm, p=0.0001). Interobserver reliability was good with an ICC of 0.76 for the left main coronary artery (95 % CI 0.64–0.85) and 0.77 for the right coronary artery (95 % CI 0.58–0.87).

Fluoroscopic projection angle: intraobserver agreement

Assuming an LAO angulation of 10°, there was no significant difference in cranial or caudal angulation comparing both measurements (mean 5±13° caudal vs. 4±14° caudal, p=0.06). The mean absolute difference between the cranial or caudal angulation for the two measurements was 5±6° (ICC 0.83, 95 % CI 0.74–0.90).

When accepting a deviation of up to 10° between the two measurements for the potential fluoroscopic projection angle, agreement concerning the fluoroscopic projection angle was present in 57 of all 64 patients (89.1 %).

Fluoroscopic projection angle: interobserver agreement

Assuming an LAO angulation of 10°, there was no significant difference in cranial or caudal angulation comparing both observers (mean 5±13° caudal vs. 7±14° caudal, p=0.22). The mean absolute difference between the cranial or caudal angulation was 6±6° (ICC 0.81, 95 % CI 0.70–0.88).

Under the assumption that a deviation of up to 10° would indicate agreement, the two observers determined equal fluoroscopic projections in 54 of all 64 patients (84.3 %).

Prosthesis size selection: intraobserver agreement

Agreement regarding prosthesis size selection was present in 48 of 64 cases (75.0 %, κ=0.83). Both measurements resulted in the recommendation of a 23-mm prosthesis in 14 cases, a 26-mm prosthesis in 29 cases, a 29-mm prosthesis in four cases and no appropriate prosthesis available in one case.

Agreement was also observed in 48 out of 64 cases when the area-derived diameter was used (75.0 %, κ=0.94).

For the circumference-derived diameter of the aortic annulus, agreement regarding prosthesis size selection was slightly superior (52 of 64 cases, 81.2 %, κ=0.91, Table 4).

Prosthesis size selection: interobserver agreement

On the basis of the mean aortic annulus diameter, the two observers reached agreement for aortic valve prosthesis size selection in 53 of 64 cases (82.8 %), resulting in close interobserver agreement (κ=0.86). The use of a 23-mm prosthesis was recommended in 12 cases, a 26-mm prosthesis in 31 cases, a 29-mm prosthesis in eight cases and no appropriate prosthesis was available in two cases.

Table 4 Interobserver and intraobserver agreement of prosthesis size selection according to the aortic annulus parameters

	Interobserver agreement (n and κ value)	Intraobserver agreement (n and κ value)
Mean diameter		
23 mm	12 (18.7 %)	14 (21.9 %)
26 mm	31 (48.4 %)	29 (45.3 %)
29 mm	8 (12.5 %)	4 (6.2 %)
No appropriate prosthesis available	2 (3.1 %)	1 (1.6 %)
	0.86	0.83
Area-derived diameter		
23 mm	7 (10.9 %)	7 (10.9 %)
26 mm	31 (48.4 %)	29 (45.3 %)
29 mm	11 (17.2 %)	10 (15.6 %)
No appropriate prosthesis available	2 (3.1 %)	2 (3.1 %)
	0.84	0.94
Circumference-derived diameter		
23 mm	6 (9.4 %)	5 (7.8 %)
26 mm	31 (48.4 %)	31 (48.4 %)
29 mm	17 (26.6 %)	13 (20.3 %)
No appropriate prosthesis available	3 (4.7 %)	3 (4.7 %)
	0.91	0.90

Table 5 Influence of the extent of aortic root calcification on the interobserver and intraobserver results of the suggested prosthesis size

Mean score	Same prosthesis size	Different prosthesis size	Significance (p value)
Interobserver			
Mean diameter	1.8±0.9	1.7±0.9	n.s. (0.72)
Area-derived diameter	1.8±0.9	1.5±0.7	n.s. (0.21)
Circumference-derived diameter	1.8±0.9	1.5±0.5	n.s. (0.39)
Intraobserver			
Mean diameter	1.8±0.8	1.8±1.1	n.s. (0.97)
Area-derived diameter	1.7±0.9	1.9±0.8	n.s. (0.46)
Circumference-derived diameter	1.8±0.9	1.6±0.5	n.s. (0.53)

Based on the area-derived diameter of the aortic annulus, agreement regarding prosthesis size selection occurred in 51 of 64 cases (79.7 %, κ=0.84, Table 4).

Based on the circumference-derived diameter of the aortic annulus, agreement regarding prosthesis size selection was found in 57 of 64 cases (89.0 %, κ=0.91).

Influence of the aortic root calcification on the accuracy of the results

The mean score of aortic root calcification was 1.8±0.9 in patients in whom the two observers were in agreement regarding prosthesis size based on the mean diameter, compared to a mean score of 1.7±0.9 in cases of disagreement (p= 0.72, Table 5). The aortic root calcification score influenced neither interobserver agreement regarding prosthesis size nor the agreement regarding the suitable fluoroscopic projection angle (Table 6).

Analysis time

The mean time required to create a multiplanar reconstruction exactly aligned with the aortic valve insertion points was 86± 22 s (range 57–127 s). The mean time for the entire analysis per patient was 4.6±1.7 min (range 3–12 min).

Table 6 Influence of the extent of aortic root calcification on the interobserver and intraobserver results of the potential fluoroscopic projection angle

Mean score	Same fluoroscopic projection angle	Different fluoroscopic projection angle	Significance (p value)
Interobserver	1.8±0.8	1.8±1.0	n.s. (0.86)
Intraobserver	1.8±0.9	1.7±0.8	n.s. (0.91)

Discussion

Accurate determination of aortic root dimensions and geometry is essential for pre-procedural evaluation of TAVI candidates by CT. Performing this measurement is not trivial and, accordingly, previous studies demonstrated limited interobserver agreement. Gurvitch et al. validated an approach based on the reconstruction of a coronal and sagittal oblique plane, an oblique plane in a three-chamber view and a double oblique transverse image of the basal ring and found a wide range of interobserver variability. The highest reproducibility was reported for the area-derived diameter and the mean diameter (ICC 0.87 and 0.80 for interobserver and greater than 0.90 for intraobserver reliability, respectively) [6]. A study by Hutter et al. showed only a fair interobserver agreement (ICC 0.39) for the mean diameter of the aortic annulus [22].

We evaluated a recently described systematic approach [19] which provides a straightforward and software-independent alignment of the imaging plane with the aortic annulus plane in CT data sets. We demonstrated that the method is fast, and excellent inter- and intraobserver reliabilities for the aortic annulus dimensions were obtained. These results and the potential choice of the prosthesis size were not influenced by the extent of aortic root calcification. Similarly, we found close intra- and interobserver agreement for determination of the distance of the coronary ostia from the aortic annulus plane which needs to be measured accurately to avoid potential obstruction of the coronary arteries [2]. Whereas some studies compared measurements of the distances of the coronary ostia from the aortic valve plane between different cardiac phases [23] or between different imaging modalities [24], our study is the first one which evaluated inter- and intraobserver reliability. The fact that measurement of this distance was more reproducible for the left coronary artery as opposed to the right remains unclear. A potential explanation is the fact that the left sinus of Valsalva seems to be narrower than the right, so that the line from the left main coronary ostium to the aortic annulus is almost orthogonal. The right coronary ostium is not as well aligned with the aortic

annulus, which makes the measurement of the distance more difficult.

A limited number of studies have evaluated the potential of CT to determine an appropriate fluoroscopic projection angle for TAVI procedures [14–17]. None of these studies systematically assessed the reproducibility of such measurements. Our results demonstrate that CT permits one to suggest a potential fluoroscopic projection angle with a high degree of intra- and interobserver reproducibility (ICC 0.81 and 0.83). The mean difference between the two observers and between the two measurements of one observer was quite small (6±6° vs. 5±6°), and such differences typically play no role in the implantation process.

The most relevant finding of our study is probably the degree of inter- and intraobserver agreement regarding prosthesis size selection. Several studies have shown that according to CT measurements, prosthesis size selection is different as compared to echocardiography-based sizing [6, 7, 20, 25]. However, no study compared interobserver or intraobserver reliability concerning the described method to measure the aortic annulus parameters. Even though we demonstrated a high inter- and intraobserver agreement, the recommended prosthesis size would have differed in 11–25 % of cases of repeated measurements. This is mainly because strict cut-off thresholds were used in our study, so that a difference of 0.1 mm would lead to different prosthesis size suggestions, and many measurement values were around the cut-off thresholds of 22.5 and 26.5 mm. In clinical practice, there is some leeway rather than a strict cut-off value and measurements would be repeated and compared to other modalities especially in cases near the threshold values. Finally, clinical determination of prosthesis size would also integrate other factors such as the extent of aortic valve calcification and annulus eccentricity [13].

Our study suffers from several limitations. We did not compare our measurement results with other imaging modalities such as TEE-based annular sizing. Rather, our intention was to evaluate the newly described method to systematically create a multiplanar reconstruction aligned with the aortic annulus plane regarding reproducibility. Further studies are needed to prospectively evaluate this method, concerning the accuracy to minimize aortic annulus to prosthesis size mismatch as well as the applicability of the suggested implantation angle.

In conclusion, stepwise alignment of a multiplanar reconstruction with the lowest insertion points of all three coronary cusps permits the rapid generation of a cross-section which is exactly aligned with the aortic annulus plane. This method provides high reproducibility when determining aortic root dimensions or suitable fluoroscopic projection angles for TAVI.

Acknowledgments The scientific guarantor of this publication is Prof. Stephan Achenbach. The authors of this manuscript declare relationships with the following companies: Stephan Achenbach received speaker honoraria from Edwards Lifesciences. This study has received funding from the W. R. Pitzer Foundation, Bad Nauheim (11-111). No complex statistical methods were necessary for this paper. Institutional review board approval was not required because it was a retrospective analysis of anonymized data sets. Written informed consent was not required for this study because it was a retrospective analysis of anonymized data sets. Methodology: retrospective, multicenter study.

References

1. Holmes DR Jr, Mack MJ, Kaul S et al (2012) 2012 ACCF/AATS/SCAI/STS expert consensus document on transcatheter aortic valve replacement. J Am Coll Cardiol 59:1200–1254
2. Masson JB, Kovac J, Schuler G et al (2009) Transcatheter aortic valve implantation: review of the nature, management, and avoidance of procedural complications. J Am Coll Cardiol Cardiovasc Interv 2:811–820
3. Hayashida K, Bouvier E, Lefèvre T et al (2012) Potential mechanism of annulus rupture during transcatheter aortic valve implantation. Catheter Cardiovasc Interv. doi:10.1002/ccd.24524
4. Blanke P, Reinöhl J, Schlensak C et al (2012) Prosthesis oversizing in balloon-expandable transcatheter aortic valve implantation is associated with contained rupture of the aortic root. Circ Cardiovasc Interv 5:540–548
5. Stabile E, Sorropago G, Cioppa A et al (2010) Acute left main obstructions following TAVI. EuroIntervention 6:100–105
6. Gurvitch R, Webb JG, Yuan R et al (2011) Aortic annulus diameter determination by multidetector computed tomography: reproducibility, applicability, and implications for transcatheter aortic valve implantation. J Am Coll Cardiol Cardiovasc Interv 4:1235–1245
7. Jilaihawi H, Kashif M, Fontana G et al (2012) Cross-sectional computed tomographic assessment improves accuracy of aortic annular sizing for transcatheter aortic valve replacement and reduces the incidence of paravalvular aortic regurgitation. J Am Coll Cardiol 59:1275–1286
8. Kempfert J, Van Linden A, Lehmkuhl L et al (2012) Aortic annulus sizing: echocardiographic vs. computed tomography derived measurements in comparison with direct surgical sizing. Eur J Cardiothorac Surg. doi:10.1093/ejcts/ezs064
9. Jabbour A, Ismail TF, Moat N et al (2011) Multimodality imaging in transcatheter aortic valve implantation and post-procedural aortic regurgitation. J Am Coll Cardiol 58:2165–2173
10. Leipsic J, Gurvitch R, LaBounty TM et al (2011) Multidetector computed tomography in transcatheter aortic valve implantation. J Am Coll Cardiol Img 4:416–429
11. Willson AB, Webb JG, LaBounty TM et al (2012) 3-dimensional aortic annular assessment by multidetector computed tomography predicts moderate or severe paravalvular regurgitation after transcatheter aortic valve replacement: a multicenter retrospective analysis. J Am Coll Cardiol 59:1287–1294
12. Binder RK, Webb JG, Willson AB et al (2013) The impact of integration of a multidetector computed tomography annulus area sizing algorithm on outcomes of transcatheter aortic valve replacement: a prospective, multicenter, controlled trial. J Am Coll Cardiol. doi:10.1016/j.jacc.2013.04.036
13. Achenbach S, Delgado V, Hausleiter J, Schoenhagen P, Min JK, Leipsic JA (2012) SCCT expert consensus document on computed tomography imaging before transcatheter aortic valve implantation

(TAVI)/transcatheter aortic valve replacement (TAVR). J Cardiovasc Comput Tomogr 6:366–380
14. Gurvitch R, Wood DA, Leipsic J et al (2010) Multislice computed tomography for prediction of optimal angiographic deployment projections during transcatheter aortic valve implantation. J Am Coll Cardiol Cardiovasc Interv 3:1157–1165
15. Binder RK, Leipsic J, Wood D et al (2012) Prediction of optimal deployment projection for transcatheter aortic valve replacement: angiographic 3-dimensional reconstruction of the aortic root versus multidetector computed tomography. Circ Cardiovasc Interv 5:247–252
16. Kurra V, Kapadia SR, Tuzcu EM et al (2010) Pre-procedural imaging of aortic root orientation and dimensions: comparison between x-ray angiographic planar imaging and 3-dimensional multidetector row computed tomography. J Am Coll Cardiol Cardiovasc Interv 3:105–113
17. Arnold M, Achenbach S, Pfeiffer I et al (2012) A method to determine suitable fluoroscopic projections for transcatheter aortic valve implantation by computed tomography. J Cardiovasc Comput Tomogr 6:422–428
18. Wuest W, Anders K, Schuhbaeck A et al (2012) Dual source multidetector CT-angiography before transcatheter aortic valve implantation (TAVI) using a high-pitch spiral acquisition mode. Eur Radiol 22:51–58
19. Achenbach S, Schuhbäck A, Min JK, Leipsic J (2013) Determination of the aortic annulus plane in CT imaging-a step-by-step approach. J Am Coll Cardiol Img 6:275–278
20. Tzikas A, Schultz CJ, Piazza N et al (2011) Assessment of the aortic annulus by multislice computed tomography, contrast aortography, and trans-thoracic echocardiography in patients referred for transcatheter aortic valve implantation. Catheter Cardiovasc Interv 77:868–875
21. Landis JR, Koch GG (1977) The measurement of observer agreement for categorical data. Biometrics 33:159–174
22. Hutter A, Opitz A, Bleiziffer S et al (2010) Aortic annulus evaluation in transcatheter aortic valve implantation. Catheter Cardiovasc Interv 76:1009–1019
23. Pontone G, Andreini D, Bartorelli AL et al (2011) Feasibility and accuracy of a comprehensive multidetector computed tomography acquisition for patients referred for balloon-expandable transcatheter aortic valve implantation. Am Heart J 161:1106–1113
24. Tamborini G, Fusini L, Gripari P et al (2012) Feasibility and accuracy of 3DTEE versus CT for the evaluation of aortic valve annulus to left main ostium distance before transcatheter aortic valve implantation. J Am Coll Cardiol Img 5:579–588
25. Messika-Zeitoun D, Serfaty JM, Brochet E et al (2010) Multimodal assessment of the aortic annulus diameter. J Am Coll Cardiol 55:186–194